



Localization and force analysis at the single virus particle level using atomic force microscopy

Chih-Hao Liu^a, Jim-Tong Horng^b, Jeng-Shian Chang^a, Chung-Fan Hsieh^c, You-Chen Tseng^a, Shiming Lin^{a,d,*}

^a Institute of Applied Mechanics, Nation Taiwan University, Roosevelt Road, Taipei 10617, Taiwan

^b Department of Biochemistry, Chang Gung University, 259 Wen-Hwa First Road, Kweishan, Taoyuan 333, Taiwan

^c Graduate Institute of Biomedical Sciences, Chang Gung University, Kweishan, Taoyuan 333, Taiwan

^d Center for Optoelectronic Biomedicine, College of Medicine, Nation Taiwan University, 1-1 Jen-Ai Road, Taipei 10051, Taiwan

ARTICLE INFO

Article history:

Received 8 November 2011

Available online 22 November 2011

Keywords:

Atomic force microscopy (AFM)

Localization

Unbinding force

Force mapping

Influenza virus

ABSTRACT

Atomic force microscopy (AFM) is a vital instrument in nanobiotechnology. In this study, we developed a method that enables AFM to simultaneously measure specific unbinding force and map the viral glycoprotein at the single virus particle level. The average diameter of virus particles from AFM images and the specificity between the viral surface antigen and antibody probe were integrated to design a three-stage method that sets the measuring area to a single virus particle before obtaining the force measurements, where the influenza virus was used as the object of measurements. Based on the proposed method and performed analysis, several findings can be derived from the results. The mean unbinding force of a single virus particle can be quantified, and no significant difference exists in this value among virus particles. Furthermore, the repeatability of the proposed method is demonstrated. The force mapping images reveal that the distributions of surface viral antigens recognized by antibody probe were dispersed on the whole surface of individual virus particles under the proposed method and experimental criteria; meanwhile, the binding probabilities are similar among particles. This approach can be easily applied to most AFM systems without specific components or configurations. These results help understand the force-based analysis at the single virus particle level, and therefore, can reinforce the capability of AFM to investigate a specific type of viral surface protein and its distributions.

© 2011 Elsevier Inc. All rights reserved.

1. Introduction

Atomic force microscopy (AFM) is a powerful tool that not only enables imaging with nanometer spatial resolution but also can determine the interaction force of a single biomolecule with pico-Newton force sensitivity and nanometer positional accuracy using functionalized probes [1,2]. In recent years, AFM imaging techniques have been used to detect and characterize the pathogen for rapid, direct, and label-free diagnostics. For example, immunocapture array or assay using immobilized antibodies have combined with AFM high-resolution imaging to detect and identify virus particles or other pathogens [3,4]. Another significant capability of AFM is to measure the interactions between biomolecules, such as ligand–receptor pairs [5–7] and specific antibody–antigen interaction [8,9]. In principle, AFM use a functionalized tips mounted on the end of a flexible cantilever to detect the biological,

chemical, and physical interactions. Functionalization techniques have made AFM a multifunctional nanotool [10–12].

So far, some AFM techniques using antibody probes are effective for detection and localization purposes. Force mapping have typically been used to map specific binding sites in living cells [13–15]. Researchers firstly use the optical microscopy to locate the cell under investigation, and then record both image and two-dimensional array of force curves over the same area of the sample. Recognition imaging microscopy is an analytical technique that uses an antibody–tethered AFM tip to simultaneously map the antigenic sites and obtain topographical images on a surface in AFM tapping mode [16–18]. However, during AFM force measurements of a few hundred nanometer sample size, such as virus particles, researchers cannot directly locate these particles using optical microscopy. Though fluorescently-labeled molecules can be used to identify the sample of interest, they need fixation processes and may interfere with the bioaffinity interaction under investigation. In addition, fluorescent light source and inverted optical microscope are needed in such experiments.

In this study, we propose a novel method without fluorescent tags for localization, obtaining force measurements, and force

* Corresponding author at: Center for Optoelectronic Biomedicine, College of Medicine, Nation Taiwan University, 1-1 Jen-Ai Road, Taipei 10051, Taiwan. Fax: +886 2 23949125.

E-mail address: til@ntu.edu.tw (S. Lin).

mapping images at the single virus particle level. The described methodology combines AFM high resolution images with specific unbinding events from force–distance curves. Based on this method, force measurements of each single virus particle were analyzed and statistically examined. In contrast to recognition imaging microscopy, we offer an alternative method for distinguishing single virus particles without considering the cantilever's spring constant and quality factor, or using an additional electronic detector. The proposed method enables efficient, specific, and repeated localization of an individual virus particle and its antibody–antigen unbinding force analysis.

2. Materials and methods

2.1. AFM images of influenza virus

Freshly cleaved mica was treated with 0.01%(wt./vol.) poly-L-lysine and left to dry [19]. The influenza A/WSN/33 (H1N1) virus in PBS was then applied onto the treated mica surface. After adsorption for 30 min, the mica was washed with distilled water to remove the unadsorbed viral sample, dried in air prior to AFM image experiments.

AFM images were obtained using a multimode scanning probe microscopy (SPI300 HV, Seiko Instruments, Japan). Commercial silicon cantilevers (SuperSharpSilicon™ SSS-SEIH, NANOSENSORS, Switzerland) with a typical tip radius of 2 nm were used in tapping mode in air. Topographic and phase images were obtained simultaneously using a resonant frequency of about 140 kHz for the probe oscillation.

2.2. AFM force measurements

A scanning probe microscope (SPM) measuring head (SMENA liquid head, NTMDT, Moscow, Russia) was used to directly measure the interaction force between influenza hemagglutinin (HA) and anti-hemagglutinin (anti-HA) monoclonal antibody (ab8262, Abcam, UK) probe in liquid environment. First, AFM silicon cantilevers (PointProbePlus, Nanosensors, Switzerland) and glass slides (Superfrost, Germany) were immersed in 5% solution of 3-aminopropyltriethoxysilane (Fluka Chemie, Switzerland) in 5% ethanol solution for 45 min, and then rinsed with a solution of 5% ethanol/95% distilled water for 10 min [9,20]. Subsequently, they were incubated with 2.5% glutaraldehyde solution in distilled water for 75 min, and rinsed with distilled water for 10 min. In the last step, AFM tips were covalently bond with 100 µg/ml anti-HA antibody solution in PBS for overnight incubation. Before AFM force measurements, glass slides were covalently bond with viral sample solution in PBS for 2 h.

All force measurements were executed at the same loading rate of 166.6 nm/s in PBS buffer (pH 7.0) in the 35 mm Petri dish. The interaction force between influenza HA and anti-HA antibody probe was measured by approaching the tip towards the sample perpendicularly. Fig. 1A and B shows the representative force–distance curves for non-specific unbinding event and specific unbinding event respectively. In contrast to the non-specific unbinding event in Fig. 1A, a clear peak can be observed in the retracting process in Fig. 1B, which indicates a specific interaction between the influenza virus surface glycoprotein HA and anti-HA antibody probe [21–23].

3. Results

3.1. AFM images of influenza virus

Fig. 2A shows the AFM height images (scanning area 5 µm × 5 µm) of the viral samples, and the virus particles appear to be predominately spherical and uniformly distributed on the surface. The higher-resolution images (Fig. 2B and C) were acquired by zooming into the square area displayed in Fig. 2A and B, respectively. In Fig. 2C, each single virus particle can be readily observed and differentiated. To investigate the dimension of a single viral particle, three particles marked by squares in Fig. 2C were zoomed in Fig. 2D–F (height images) and Fig. 2G–I (phase images). These images were then analyzed by AFM imaging software to determine the mean diameter of virus particles. Over 20 single viral particles were measured, and their average diameter from the AFM image was 104 ± 17.6 nm (mean ± SD, n = 21), in agreement with the size estimated from electron microscopy or cryo-electron microscopy [24,25].

3.2. Three-stage localization methodology

The localization method for single virus particle can be divided into three stages. The principle is to use the specific unbinding event between the influenza HA and anti-HA antibody probe to calculate appropriate measuring areas and measuring points, in accordance with different stages of localization and the geometric measurements of virus particles and surface antigens. All localization processes were performed at the same loading rate of 166.6 nm/s in PBS at pH 7.0. Schematic diagrams of the three localization stages are shown in Fig. 3A–C, respectively, and the corresponding representative AFM images are presented in Fig. 3D–F. The detailed methodology is described as follows.

3.2.1. Stage 1

The objective in Stage 1 is to determine the approximate location of one virus particle in the measuring area on a micrometer

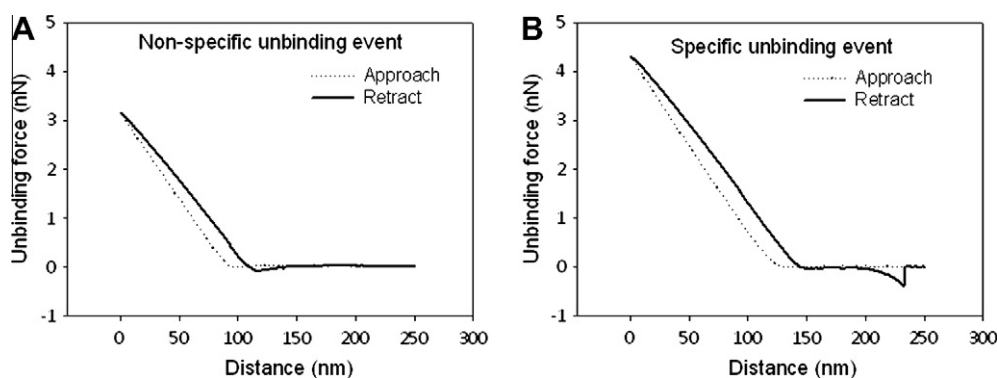


Fig. 1. Representative force–distance curves with non-specific unbinding event and specific unbinding event. (A) Typical force–distance curve with non-specific unbinding event. There is no any peak in the retracting process; (B) typical force–distance curve with specific unbinding event. A peak in the retracting process indicates a specific interaction between the viral surface glycoprotein hemagglutinin (HA) and the anti-HA antibody probe.

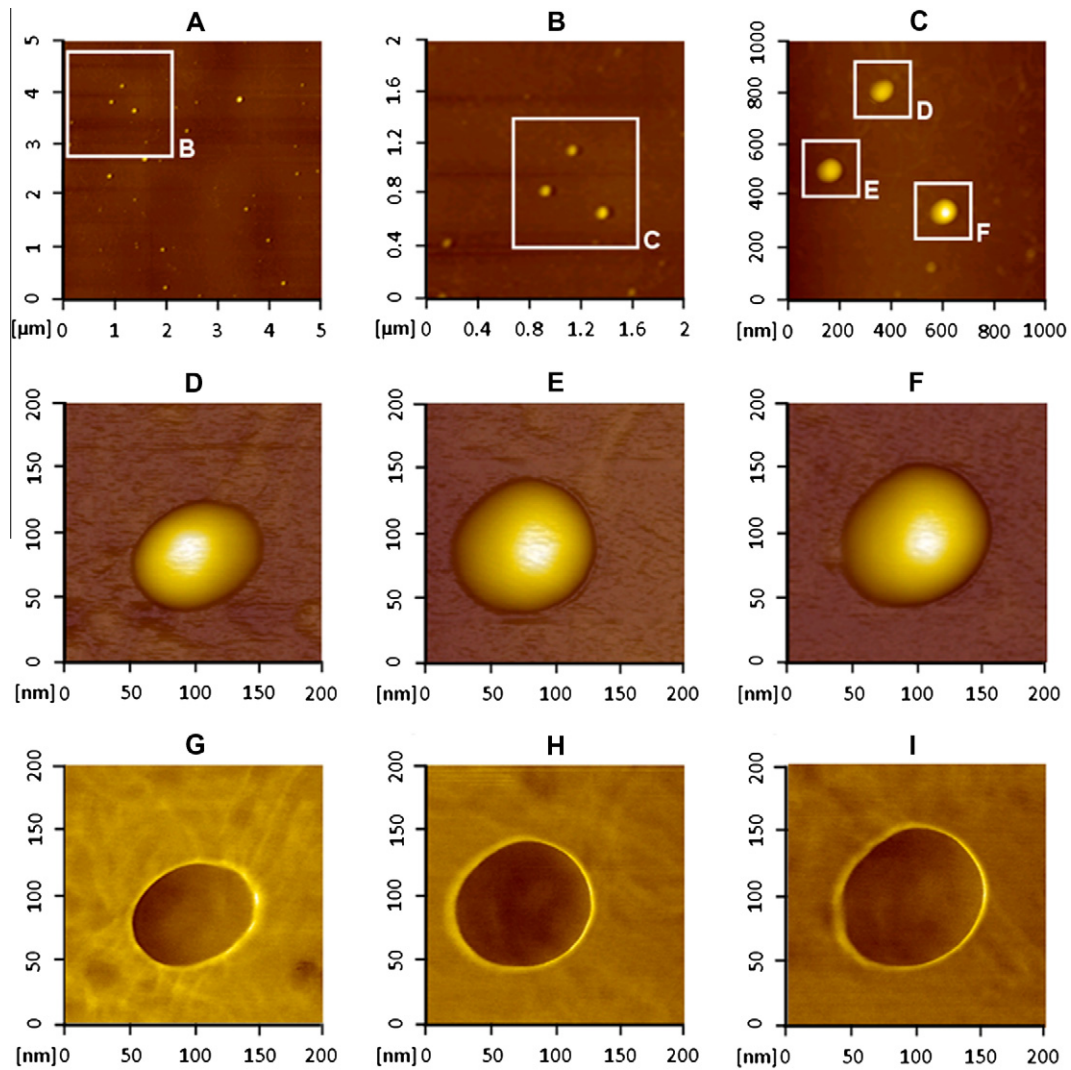


Fig. 2. AFM topographic images (top and middle row) and phase images (bottom row) of the influenza virus on mica. (A) Two-dimensional topographic images (scanning area: $5 \mu\text{m} \times 5 \mu\text{m}$); (B) (scanning area: $2 \mu\text{m} \times 2 \mu\text{m}$) and (C) (scanning area: $1 \mu\text{m} \times 1 \mu\text{m}$) are two-dimensional topographic images which acquired by zooming into the square area in (A) and (B) respectively; (D–F) three-dimensional high-resolution images (scanning area: $200 \text{ nm} \times 200 \text{ nm}$) by zooming into the three squares in (C); (G–I) phase images of (D–F) respectively.

scale by observing the force–distance curves on measuring points. Researchers know that the measuring point with specific unbinding event indicated the location of specific interaction between influenza surface antigen HA and anti-HA antibody probe, thus confirming the position of a virus particle. In general, virus particles are randomly covalently bound to a chemically modified glass slide. Designing a larger measuring area may facilitate the inclusion of more virus particles; however, a larger area lowers the binding possibility between the antibody probe and virus particles, which results from the fact that the size of virus particle is much smaller in a larger area, and thus necessitates more measuring points or longer measuring time to sense the approximate position of one virus particle. In this study, the measuring area in Stage 1 was configured to have a grid of 5×5 measuring points in $1 \mu\text{m}^2$, and any specific binding point can be used as the center point of the measuring area in Stage 2 (Fig. 3A and D).

3.2.2. Stage 2

The objective in Stage 2 is to reduce the measuring area to the size of one virus particle. Contemplating the distribution of the influenza virus surface antigen HA [25], we considered that the specific unbinding event in Stage 1 may not have actually been

located at the center of the virus particle surface. To ensure that the measuring area in Stage 2 included a complete single virus particle, we used the average virus diameter obtained from image experiments, and extended the area a further 100 nm outwards from the centre point with yellow color in Stage 2 (Fig. 3B and E). Therefore, the measuring area in Stage 2 was 200 nm^2 .

In the proposed method, an appropriate number of measuring points indicates that there is sufficient resolution to identify the absolute location of one virus particle. The previous studies of antibody–antigen interaction show that the probability of specific binding is approximately 0.1–0.4 [8,22,26,27]. If the number of measuring points is too low (using 36 points as an example), a randomly selected area of 100 nm^2 would include only four measuring points on the virus particle surface (Fig. 3G). In such circumstances, we may be unable to obtain enough unbinding events to determine the location of the virus particle. If there are two adjacent virus particles in the measurement area, insufficient resolution will make it impossible to accurately identify the locations of the two particles, as shown in Fig. 3G. Using the grid mode for force measurements provided by NT-MDT Nova software, 64 measuring points can be designed. This means that a randomly selected 100 nm^2 measuring area will include a maximum of 16 specific

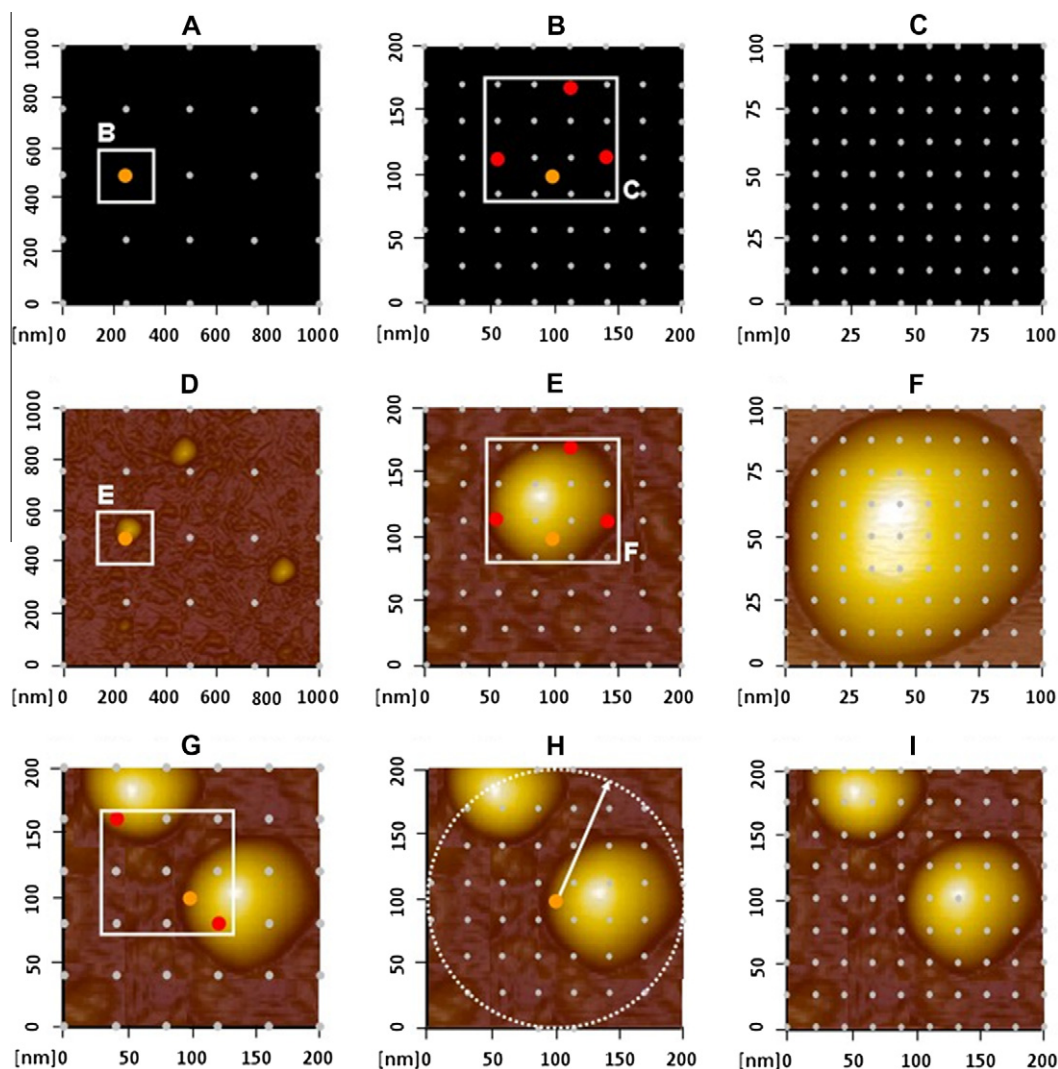


Fig. 3. Schematics of the three-stage localization method. All gray points indicate the locations on which antibody probe approached. The bolder orange and red points represent the locations which specific interaction occurred. (A) Stage 1 (measuring area: $1 \mu\text{m} \times 1 \mu\text{m}$; measuring points: 25). One specific unbinding event occurred in 25 approach points, and this point was then used as the center point of the measuring area in Stage 2; (B) stage 2 (measuring area: $200 \text{ nm} \times 200 \text{ nm}$; measuring points: 64). Measuring area in Stage 2 was designed by zooming into the square area in (A). Using the grid mode for force measurements, 64 measuring points can be configured in this stage; (C) stage 3 (measuring area: $100 \text{ nm} \times 100 \text{ nm}$; measuring points: 100). Measuring area in Stage 3 was designed by selecting the maximum specific interaction points within $100 \text{ nm} \times 100 \text{ nm}$ area in (B); (D–F) representative images of (A–C), respectively. These figures used AFM topographic images to explain the three-stage localization method; (G) representative image of (B) using 36 measuring points as an example; (H) representative image of (B) using customized software for accelerating the localization process; (I) representative image of (B) using the minimum resolution of 10 nm to determine the location of virus particle. (For interpretation of the references to colour in this figure legend, the reader is referred to the web version of this article.)

unbinding events. After 64 measurements, an area of 100 nm^2 that includes the maximum specific binding points can be used as the measuring area of the Stage 3. Notice that the specific binding point with orange color from Stage 1 is still considered as one specific binding point in Stage 2.

This study used customized software to define the location of measuring points for the purpose of accelerating the localization process (Fig. 3H). First, we used the center point of Stage 2, where the specific unbinding event was recognized in Stage 1, to draw a circle with a diameter of 100 nm ; because this diameter is the mean value of the virus particle, we estimated that many virus particles would fall within this encircled region. Next, the remaining measuring points outside of the circle were removed, and therefore 44 measuring points were used to achieve absolute localization of the virus particles. Additionally, the measuring area within a 100 nm radius circle, 78% of a square measuring area with a side length of 200 nm , may reduce the specific binding possibility of non-target virus particles, thus providing more accurate localization results.

3.2.3. Stage 3

After the localization process in Stages 1 and 2 had been completed, we assumed in Stage 3 that the 100 nm^2 measuring area included a complete virus particle. Considering that the adjacent distance between two HA was approximately 10 nm [25], we used 100 measuring points (10×10 points) in this stage (Fig. 3C and F). After 100 approach cycles, we can obtain the AFM measurements of a single influenza virus particle.

In Stages 2, if we directly use the minimum resolution of 10 nm to determine the location of the virus, although we could obtain more complete virus particle data from the measuring area (200 nm^2), the number of measuring points would increase to 425 (Fig. 3I). This means that measuring time would increase by 2.5 times. We would also be unable to distinguish adjacent virus particles.

3.2.4. Statistical analysis

The unbinding force of one virus particle was calculated from 100 force–distance curves. To ensure that the result of each virus

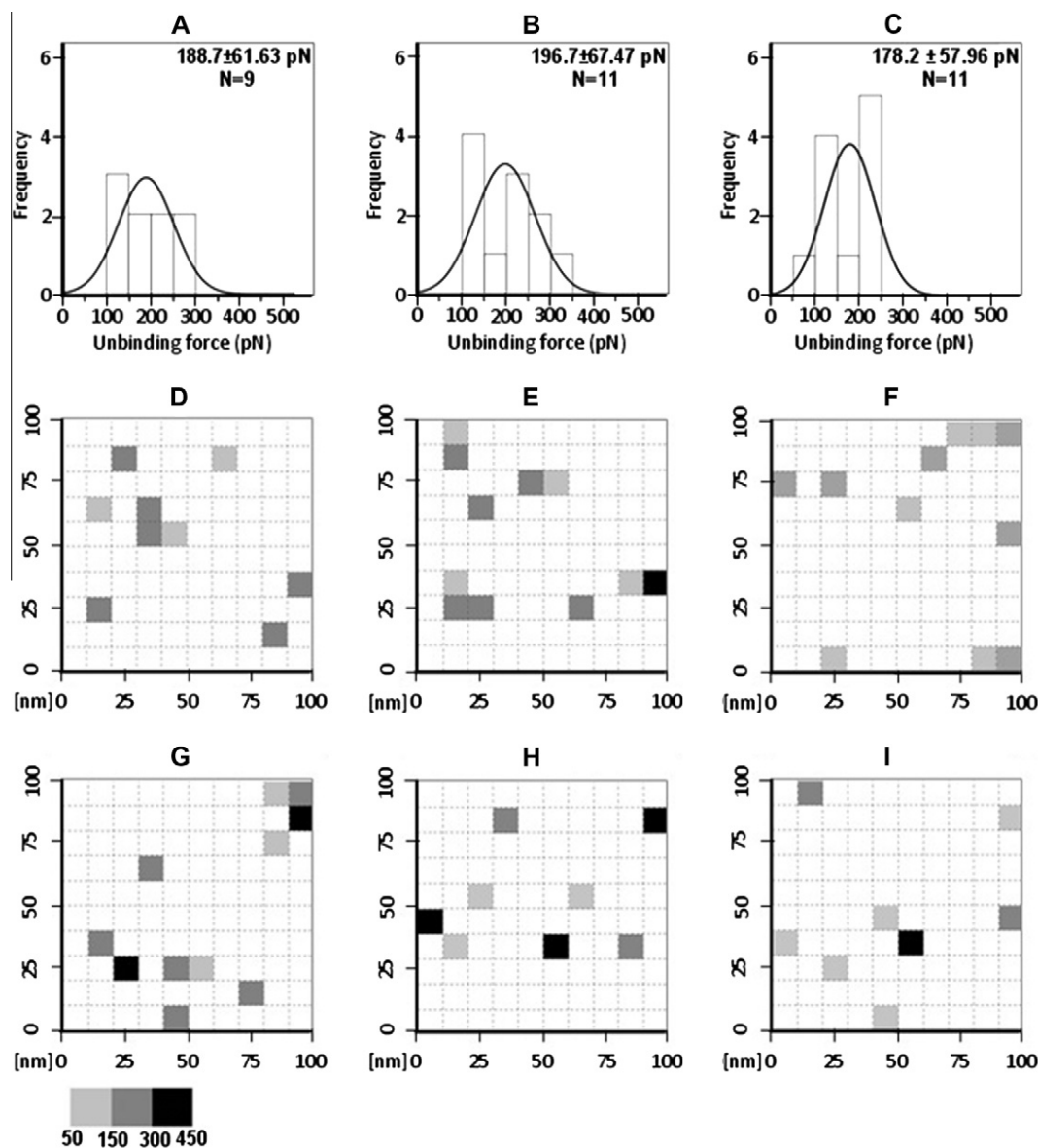


Fig. 4. (A–C) Histograms and normal curve distributions of the unbinding force measurements from three virus particles, performed at the same loading rate of 166.6 nm/s with a grid of 10×10 points in the 100 nm^2 in PBS pH 7.0; (D–F) the corresponding force mapping images to (A–C), respectively. All unbinding forces are presented in gray-level images; (G–I) the congruent force mapping images of three localized virus particles obtained on different days.

particle obtained from the localization process in Stages 1–3 showed consistent measurements, a one-way analysis of variance (ANOVA) was used to analyze differences among virus particles. The AFM measurements of each virus particle were checked for normality and homogeneity by Kolmogorov–Smirnov test and Levene test respectively. A p -value of 0.05 was considered statistically significant. Finally, ANOVA with Tukey's post hoc tests using SPSS software was conducted to evaluate the hypothesis that the mean unbinding forces among virus particles are equal under the criteria mentioned above.

3.3. Repeatability test of the proposed localization method

To confirm the repeatability of the proposed method, three consecutive measurements were performed for different localized virus particles. Supplemental Fig. 1 shows the results of unbinding forces (mean \pm SE) from two virus particles in location A (211.9 ± 16.69 , 241.4 ± 17.62 and 210.9 ± 14.32 pN) and location B (223.8 ± 18.54 ,

224.8 ± 23.61 and 193.5 ± 23.05 pN), respectively. These data were examined using one-way ANOVA, and the statistical analyses show no significant differences among measurements in the two virus particles ($p < 0.05$). This demonstrated the repeatability of the force measurements using the proposed method, and that serial force measurements did not remove the anti-HA antibody and influenza virus from the probe surface and substrate, respectively.

3.4. Force measurements and force mapping images of the localized virus particles

In the third localization step, each virus particle was measured with a grid of 10×10 points in the 100 nm^2 . The 100 force–distance cycles were analyzed to quantify the unbinding force between anti-HA antibody and HA protein of one virus particle, and the specific unbinding events in 100 cycles can be used to map the distribution of HA spikes on the virus surface. Fig. 4A–C shows histograms of unbinding force measurements from three virus

particles in one experiment, and all histograms are well fit by Gaussian (normal) distributions. Further, Fig. 4D–F displays the corresponding force mapping images to Fig. 4A–C, respectively, and Fig. 4G–I presents the congruent results obtained on different days. All unbinding forces in Fig. 4D–I are presented in gray-level images. As shown in Fig. 4D–I, the specific binding spots represent the locations of HA on the influenza virus envelope observed by the anti-HA antibody probe, and the binding probabilities among images are approximate to 10 percent in 100 force cycles. Data collected from 20 virus particles under same criteria on different days with new tips and samples resulted in the similar force distributions, yielding an unbinding force of 207.1 ± 34.48 pN (mean \pm SD) and a binding probability of 10.7%. In addition, the distribution of HA are irregularly distributed in all force mapping images, which is in agreement with the prior cryoelectron tomography [25].

4. Discussion

This paper first shows high-resolution imaging of the influenza virus, and then proposes a novel label-free method for conducting localization and force measurements at the single virus particle level. To validate the proposed methodology, the mean unbinding forces of the localized virus particles were statistically evaluated, and no significant differences were observed. In addition, the repeatability of this method was demonstrated. Based on the proposed method and performed analysis, several observations can be drawn from the results, as follows: this study presents the unbinding force between anti-HA and HA interactions of the influenza virus at the particle level. The unbinding force obtained at the same loading rate of 166.6 nm/s in PBS at pH 7.0 was 207.1 ± 34.48 pN (mean \pm SD). This finding is compatible with the antigen/antibody interactions of previous reports [8,22]. To our knowledge, this work is the first report on the spatially resolved force mapping images of virus particles. These images show a similar binding probability among virus particles, and the mean binding probability was 10.7%. This result indicates that the interaction possibility between the HA antigen and its antibody among virus particles is consistent and repeatable under the proposed method and experimental criteria. Moreover, the force mapping images reveal that the HA recognized by the antibody probe were dispersed on the whole surface of individual virus particles, which is additional evidence to support the repeatability of the proposed localization method.

The method should lead to more effective finding of the virus sample to be measured, thus accelerating the experimental process. This approach could also be implemented on most AFM instruments without considering specific probes, microscopic structures, and additional electronic equipments. Generally, the proposed method will be useful to systematically obtain AFM force measurements on virus particles as units. This contributes to the analysis of pre- and post-processing differences in objects to be measured, which benefits the diagnosis and evaluation of treatment effects. Specifically, this research could serve to reinforce the capability of AFM to analyze specific types of viral surface proteins and their distribution on the virus surface, and the present findings also give credence to this notion. In addition, the three-stage approach process can be used in combination with commercial or self-produced software to facilitate automatic approaching, which is convenient for researchers to reduce the additional time for selection of measuring points in manual approaches. However, this localization strategy can be improved to more rapidly determine the absolute location of virus particles in the measuring area. Further research with different viral samples is also recommended to confirm the utility of the proposed method. Adding another probe through a two-probe system structure may facilitate both

rapid image scanning and force measurements at the single virus particle level [28].

Appendix A. Supplementary data

Supplementary data associated with this article can be found, in the online version, at doi:10.1016/j.bbrc.2011.11.065.

References

- [1] G. Binnig, C.F. Quate, C. Gerber, Atomic force microscope, *Phys. Rev. Lett.* 56 (1986) 930–933.
- [2] Y.G. Kuznetsov, A.J. Malkin, R.W. Lucas, M. Plomp, A. McPherson, Imaging of viruses by atomic force microscopy, *J. Gen. Virol.* 82 (2001) 2025–2034.
- [3] S.R. Nettikadan, J.C. Johnson, C. Mosher, E. Henderson, Virus particle detection by solid phase immunocapture and atomic force microscopy, *Biochem. Biophys. Res. Commun.* 311 (2003) 540–545.
- [4] J.L. Huff, M.P. Lynch, S. Nettikadan, J.C. Johnson, S. Vengasandra, E. Henderson, Label-free protein and pathogen detection using the atomic force microscope, *J. Biomol. Screen.* 9 (2004) 491–497.
- [5] G.U. Lee, D.A. Kidwell, R.J. Colton, Sensing discrete streptavidin-biotin interactions with atomic force microscopy, *Langmuir* 10 (1994) 354–357.
- [6] E.L. Florin, V.T. Moy, H.E. Gaub, Adhesion forces between individual ligand-receptor pairs, *Science* 264 (1994) 415–417.
- [7] P.P. Lehenkari, M.A. Horton, Single integrin molecule adhesion forces in intact cells measured by atomic force microscopy, *Biochem. Biophys. Res. Commun.* 259 (1999) 645–650.
- [8] P. Hinterdorfer, W. Baumgartner, H.J. Gruber, K. Schilcher, H. Schindler, Detection and localization of individual antibody-antigen recognition events by atomic force microscopy, *Proc. Nat. Acad. Sci. USA* 93 (1996) 3477–3481.
- [9] S. Allen, X.Y. Chen, J. Davies, M.C. Davies, A.C. Dawkes, J.C. Edwards, C.J. Roberts, J. Sefton, S.J.B. Tendler, P.M. Williams, Detection of antigen-antibody binding events with the atomic force microscope, *Biochemistry* 36 (1997) 7457–7463.
- [10] D. Fotiadis, S. Scheuring, S.A. Muller, A. Engel, D.J. Muller, Imaging and manipulation of biological structures with the AFM, *Micron* 33 (2002) 385–397.
- [11] P. Hinterdorfer, Y.F. Dufrene, Detection and localization of single molecular recognition events using atomic force microscopy, *Nature Methods* 3 (2006) 347–355.
- [12] D.J. Muller, Y.F. Dufrene, Atomic force microscopy as a multifunctional molecular toolbox in nanobiotechnology, *Nature Nanotechnol.* 3 (2008) 261–269.
- [13] M. Grandbois, W. Dettmann, M. Benoit, H.E. Gaub, Affinity imaging of red blood cells using an atomic force microscope, *J. Histochem. Cytochem.* 48 (2000) 719–724.
- [14] N. Almqvist, R. Bhatia, G. Primbs, N. Desai, S. Banerjee, R. Lal, Elasticity and adhesion force mapping reveals real-time clustering of growth factor receptors and associated changes in local cellular rheological properties, *Biophys. J.* 86 (2004) 1753–1762.
- [15] O. du Roure, A. Saez, A. Buguin, R.H. Austin, P. Chavrier, P. Silberzan, B. Ladoux, Force mapping in epithelial cell migration, *Proc. Nat. Acad. Sci. USA* 102 (2005) 2390–2395.
- [16] O.H. Willemsen, M.M.E. Snel, K.O. van der Werf, B.G. de Groot, J. Greve, P. Hinterdorfer, H.J. Gruber, H. Schindler, Y. van Kooyk, C.G. Figdor, Simultaneous height and adhesion imaging of antibody-antigen interactions by atomic force microscopy, *Biophys. J.* 75 (1998) 2220–2228.
- [17] A. Raab, W.H. Han, D. Badt, S.J. Smith-Gill, S.M. Lindsay, H. Schindler, P. Hinterdorfer, Antibody recognition imaging by force microscopy, *Nature Biotechnol.* 17 (1999) 902–905.
- [18] C. Stroh, H. Wang, R. Bash, B. Ashcroft, J. Nelson, H. Gruber, D. Lohr, S.M. Lindsay, P. Hinterdorfer, Single-molecule recognition imaging-microscopy, *Proc. Nat. Acad. Sci. USA* 101 (2004) 12503–12507.
- [19] S. Lin, C.K. Lee, S.Y. Lee, C.L. Kao, C.W. Lin, A.B. Wang, S.M. Hsu, L.S. Huang, Surface ultrastructure of SARS coronavirus revealed by atomic force microscopy, *Cell Microbiol.* 7 (2005) 1763–1770.
- [20] A. Vincikier, P. Gervasoni, F. Zaugg, U. Ziegler, P. Lindner, P. Groscurth, A. Pluckthun, G. Semenza, Atomic force microscopy detects changes in the interaction forces between GroEL and substrate proteins, *Biophys. J.* 74 (1998) 3256–3263.
- [21] H. Nakajima, Y. Kunioka, K. Nakano, K. Shimizu, M. Seto, T. Ando, Scanning force microscopy of the interaction events between a single molecule of heavy meromyosin and actin, *Biochem. Biophys. Res. Commun.* 234 (1997) 178–182.
- [22] S. Lin, Y.-M. Wang, L.-S. Huang, C.-W. Lin, S.-M. Hsu, C.-K. Lee, Dynamic response of glucagon/anti-glucagon pairs to pulling velocity and pH studied by atomic force microscopy, *Biosensors and Bioelectronics* 22 (2007) 1013–1019.
- [23] M.Q. Hu, J.K. Wang, J.Y. Cai, Y.Z. Wu, X.P. Wang, Nanostructure and force spectroscopy analysis of human peripheral blood CD4(+) T cells using atomic force microscopy, *Biochem. Biophys. Res. Commun.* 374 (2008) 90–94.
- [24] F.P. Booy, R.W.H. Ruigrok, E.F.J. van Bruggen, Electron microscopy of influenza virus: a comparison of negatively stained and ice-embedded particles, *J. Mol. Biol.* 184 (1985) 667–676.

- [25] A. Harris, G. Cardone, D.C. Winkler, J.B. Heymann, M. Brecher, J.M. White, A.C. Steven, Influenza virus pleiomorphy characterized by cryoelectron tomography, *Proc. Nat. Acad. Sci. USA* 103 (2006) 19123–19127.
- [26] G. Kada, L. Blayney, L.H. Jeyakumar, F. Kienberger, V.P. Pastushenko, S. Fleischer, H. Schindler, F.A. Lai, P. Hinterdorfer, Recognition force microscopy/spectroscopy of ion channels: applications to the skeletal muscle Ca²⁺ release channel (RYR1), *Ultramicroscopy* 86 (2001) 129–137.
- [27] F. Kienberger, G. Kada, H. Mueller, P. Hinterdorfer, Single molecule studies of antibody–antigen interaction strength versus intra-molecular antigen stability, *J. Mol. Biol.* 347 (2005) 597–606.
- [28] E.T.E. Tsunemi, K. Kobayashi, K. Matsushige, H. Yamada, Development of dual-probe atomic force microscopy system using optical beam deflection sensors with obliquely incident laser beams, *Rev. Sci. Inst.* 82 (2011).